Measurement of the effect of lattice strain on magnetic interactions and orbital splitting in $CaCuO_2$ using resonant inelastic x-ray scattering

M. Minola,[1] L. Hozoi,[2] D. Di Castro,[3] R. Felici,[4] M. Moretti Sala,[5,*] A. Tebano,[3] G. Balestrino,[3] G. Ghiringhelli,[5] Jeroen van den Brink,[2] and L. Braicovich[5]

[1]*CNISM and Dipartimento di Fisica, Politecnico di Milano, piazza Leonardo da Vinci 32, I-20133 Milano, Italy*
[2]*IFW Dresden, Helmholtzstr. 20, D-01069 Dresden, Germany*
[3]*CNR-SPIN and Dipartimento di Ingegneria Civile e Ingegneria Informatica, Università di Roma Tor Vergata, Via del Politecnico 1, I-00133 Roma, Italy*
[4]*European Synchrotron Radiation Facility, 6 rue Jules Horowitz, F-38043 Grenoble, France*
[5]*CNR-SPIN and Dipartimento di Fisica, Politecnico di Milano, piazza Leonardo da Vinci 32, I-20133 Milano, Italy*

(Received 31 October 2012; revised manuscript received 30 January 2013; published 19 February 2013)

The energy of magnetic and orbital excitations of copper-oxide systems have been assessed in bulk materials, but little is known about how they change in thin films or heterostructures. Although in these samples the epitaxial strain is known to alter important physical properties, such as T_c, the actual relation to fundamental excitations remains to be established. Here we determine how the magnetic interactions and orbital splitting scale with lattice constant under strain in the prototypical insulating cuprate $CaCuO_2$. We extract the scaling power laws both experimentally, using Cu L_3 resonant inelastic x-ray scattering, and theoretically, with *ab initio* quantum chemical calculations. This combined approach quantifies the large impact of small lattice variations on the magnetic and orbital energy scales and opens the way to the production of strain-engineered samples.

DOI: 10.1103/PhysRevB.87.085124 PACS number(s): 78.70.En, 71.15.−m, 74.25.−q, 78.70.Ck

I. INTRODUCTION

Given the importance of high-T_c superconductivity the fundamental energy scales of bulk copper-oxide materials have been studied in depth for the last 25 years, and they are known in detail.[1] The recent progress in epitaxial growth and its integration with superconducting materials calls now for the extension of these studies to very thin films and heterostructures. One ineludible factor there is the strain induced on samples grown on any suitable substrate. Looking at other important 3*d* transition metal systems it is already known that strain affects various physical properties such as ferroelectricity in $SrTiO_3$,[2] phase transitions in $BiFeO_3$,[3] and *d*-orbital response in $LaNiO_3$.[4] In superconducting cuprates the critical temperature T_c typically increases upon in-plane lattice compression and decreases under tensile strain.[5]

In this paper we clarify the basic connection between the change of lattice parameter due to strain and the energy scales of the magnetic and orbital excitations. Although they both depend on the covalency of Cu-O bonds, the latter depends on the ionic crystal field as well. The relation on the interatomic distances is thus expected to be significantly different, and a joint study on the very same sample can provide reliable insight valid for the whole class of layered cuprates. We have chosen $CaCuO_2$ (hereafter called CCO)[6] and combined resonant inelastic x-ray scattering (RIXS)[7,8] with theoretical quantum chemistry calculations.[9,10] In particular we show that the lattice parameter (a) dependence is expressed by the power law $a^{-8.2}$ for magnetic excitations and $a^{-4.1}$ to $a^{-3.95}$ for orbital energies, depending on the considered orbital.

The choice of CCO is due to the simplicity of its "infinite layer" structure. In fact CCO is an antiferromagnetic insulator with a simple stacking of CuO_2 planes[6] without apical oxygens [see Fig. 1(a)], which makes it a convenient model system.[11,12] We take advantage of the possibility to control the strain by growing epitaxially a thin film on a suitable substrate with a lattice mismatch (see also the Appendix). The control is obtained by choosing the thickness of the film, as shown pictorially for the case of tensile strain in the cartoon of Fig. 1(b). Going far from the interface, where the CCO sample is expanded, the system relaxes, so that films having different thickness have a different average lattice parameter. We note here that in the following we are interested in the average lattice parameter and not in the details of relaxation. The results give direct information on the magnetic energy scale and the orbital one in "pure" CuO_2 planes, i.e., without apical oxygens. However they will also constitute a benchmark for superconducting systems having apical oxygens. In particular this could be done for the widely studied 123 systems (e.g., $YBa_2Cu_3O_7$), which have oxygen pyramids, and 214 systems (e.g., $La_{1.85}Sr_{0.15}CuO_4$), which have oxygen octahedra. Moreover CCO-based systems can also become superconductors when apical oxygens are present: This is the case of artificially engineered heterostructures[13] or samples with randomly distributed planar defects (stacking faults) that may occur in bulk systems stabilized by strontium.[14,15]

The present experimental work exploits some of the unique possibilities offered by RIXS. This is a second order process in which the sample is excited at an absorption resonance and decays by emitting a lower energy photon. Thus the transferred energy (and momentum) characterize the excitation of the system in the final state.[8] In this way it is possible to identify both the magnetic[16–18] and the orbital excitations[19] in the same measured spectrum, i.e., in strictly comparable conditions. This is a unique feature of RIXS. In particular, when RIXS is performed at the Cu L_3 edge (Cu $2p_{3/2}$ absorption threshold), with two dipole allowed transitions it is possible to excite dipole forbidden excitations between Cu 3*d* states of different symmetries. Another unequalled characteristic of modern RIXS is the possibility to get this information in very thin films (down to a few monolayers in

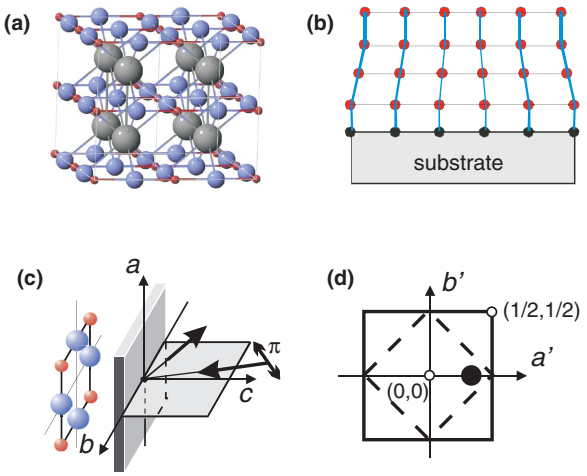

FIG. 1. (Color online) (a) Infinite-layer structure of $CaCuO_2$ (Cu in red, O in blue, and Ca in gray). (b) Pictorial illustration of the effect of epitaxial strain: The region near the substrate is strained while the system progressively relaxes towards the top of the film. In this way films with different thickness have different average lattice parameter. (c) Experimental RIXS geometry: The sample (001) surface is mounted vertically and can be rotated around the b axis to change the momentum transfer along the a axis. (d) The 2D reciprocal lattice with the nuclear (solid line) and the magnetic (dashed line) first Brillouin zone; the solid circle indicates the point chosen for the RIXS measurements.

the case of cuprates) and on relatively small surface areas (at present about $5 \times 50\ \mu m^2$), thus offering the opportunity to study superlattices and, potentially, individual interfaces. This extreme sensitivity contrasts the well-known limitations of inelastic neutron scattering that are commonly used to study the magnon dispersion in cuprates but requires massive single crystals of several tens of grams.

II. METHODS AND EXPERIMENTAL

A. Method

We present the general concepts at the basis of the method used here. As anticipated above, the strain effect is due to the variation with the distance of the overlap integrals. Thus in general the energy eigenvalues depend on the distance as $(a_0 + \delta a)^{-n}$ (see Refs. 20 and 21) where a_0 is the lattice parameter of relaxed CCO, δa is the strain-induced variation, and n is the exponent we are looking for. Diffraction shows that the maximum of δa is slightly above 1% so that it is safe to develop in series, i.e.,

$$\frac{\delta E}{E_0} = -n \cdot \frac{\delta a}{a_0}. \tag{1}$$

The error due to the series truncation is negligible: with $n = 4$ the worst case gives with Eq. (1) an effect on energy of 4.9% in place of 5% (orbital excitations) and of 9.5% in place of 10% (magnetic excitations).

Thus the experiment is done in a linear regime and this has relevant consequences. First of all the linearity ensures that the average energy shift due to the strain can be directly compared with the theoretical energy shift calculated in correspondence with the average change δa measured with diffraction. Indeed we can safely obtain relevant information without addressing the difficult problem of the strain distribution within the sample. This is a great simplification, provided the average energy shift is measured with sufficient accuracy. Also in this connection the smallness of the effect helps a lot: In fact extensive numerical simulations showed that the shift of the peak position of a spectral feature is a good indicator of the shift of the average energy, and we estimated that the maximum error is 20–25 meV. This is possible only because the shift in energy is small with respect to the energy width of the spectral components. Thus we determined the peak position directly on the spectra with the help of a Voigt fitting, as done for the magnon in Ref. 16. An example will be given while presenting the data in Fig. 2. Finally the simulations demonstrate that the

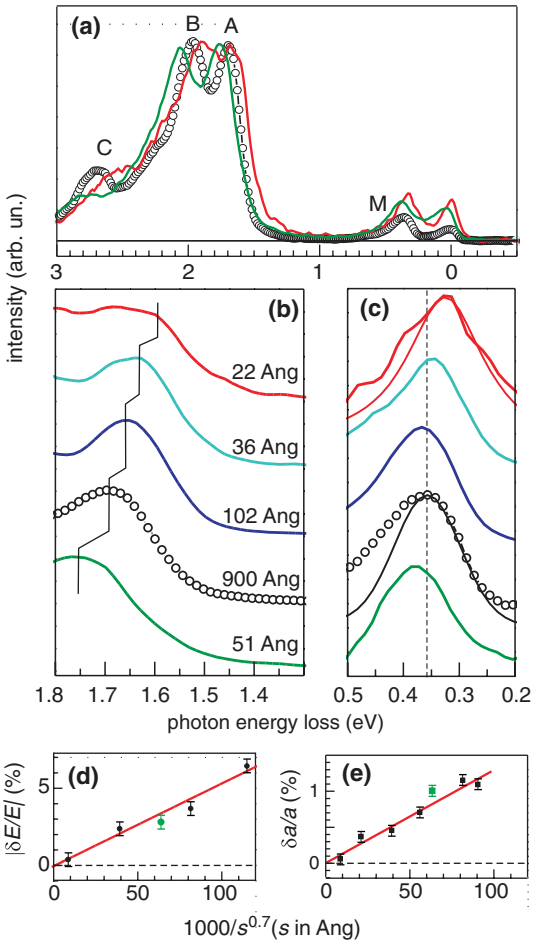

FIG. 2. (Color online) (a) Cu L_3 RIXS spectra as a function of strain; the fully relaxed, reference case (open dots) is compared with the maximum compressive (green) and tensile (red) strained cases. (b)(c) Thickness dependence of the RIXS spectra in the region of peak A, corresponding to the excitation from $x^2 - y^2$ to xy orbital with energy E_{xy}, and peak M, single magnon excitation. The thin lines in panel (c) are two examples of Voigt fitting of the magnon peaks; the higher measured tail at the right is due to phonons and that at the left to multimagnons, as explained in Ref. 16. (d)(e) Dependence of the orbital excitation energy E_{xy} and of the average lattice parameter a on film thickness s; black symbols are for tensile strain ($SrTiO_3$ substrate, various thickness values) and green symbols for compressive strain ($LaAlO_3$ substrate) changed in sign.

average values are very robust, i.e., they have little sensitivity to the details of the relaxation process across the sample. On one side this strongly supports the reliability of the present results and on the other side it shows that a study of relaxation is out of the possibilities of the present approach.

B. Experimental

The CCO samples were thin films epitaxially grown by pulsed laser deposition as described in Ref. 22 on (100) $SrTiO_3$ (STO) ($a = 3.905$ Å) substrates to create tensile strain and on (100) $LaAlO_3$ (LAO) ($a = 3.78$ Å) to achieve compressive strain, given that the lattice parameter of relaxed CCO is in between those of the two substrates ($a = 3.84$ Å). Different strain conditions are obtained by growing films with different thicknesses as already explained. This approach calls for an accurate characterization described in the Appendix.

The Cu L_3 RIXS measurements were carried out at the ADRESS beamline[23] of the Swiss Light Source at the Paul Scherrer Institute with the SAXES spectrometer.[24] The system ensures a combined linewidth at the Cu L_3 edge of 130 meV and high sensitivity. Each spectrum took two hours of accumulation except for that of the thinnest sample (22 Å thick) which took about five hours. Moreover in this film the observed roughness is not negligible, and RIXS features are slightly less pronounced than in the other cases. The overall geometry of the experiment [shown in Fig. 1(c)] is standard[16,17] and only a few points need to be stressed. The goal is to maximize the sensitivity to magnetic excitations (magnons) in the final state, since these are the smallest features we are dealing with, as is clear from Fig. 2(a). To this end we have chosen a large momentum transfer in the (0,0) → (1,0) direction, which gives around the maximum displacement of the magnon from the elastic contribution. Moreover accordingly to Ref. 25 we have maximized the magnon sensitivity by choosing π polarized incoming x rays and near normal incidence. More precisely the scattering angle is 130° (included angle 50°), with incidence at 110° from the surface and grazing emission (20° from the surface). This setup gives a transferred momentum along the surface, i.e., along the CuO_2 planes, corresponding to 0.43 r.l.u. [0.86 of the distance between (0, 0) and the (1, 0) point at the Brillouin zone (BZ) boundary]. As mentioned above, all RIXS measurements were done at 15 K in order to reduce thermal scattering.

III. RESULTS AND DISCUSSION

A. RIXS data

An overview of the strain effect is offered by Fig. 2(a) where the spectra of CCO under tensile (in red) and compressive strain (in green) are compared with a sample (open dots) having sufficient thickness (1000 Å) to be considered as a relaxed reference case within the sensitivity of the measurements. The effects on RIXS spectra are evident: All features shift to lower energies under tensile strain and to higher energies under compression, which implies that both magnetic and orbital energies decrease when the lattice constant increases. The RIXS results not only show this trend, which is qualitatively expected from the distance dependence of the matrix elements, but, more importantly, they allow for a quantitative analysis, once the spectral features are assigned and tracked as a function of the lattice parameter.

In Fig. 2(a) the magnon excitation (labeled M) is identified around 350 meV consistently with other cuprates.[16] One also finds that the orbital excitations consist of three separate structures, corresponding to the transitions of the Cu $3d^9$ hole from its $x^2 - y^2$ ground state to the xy orbital (peak A), the yz and zx orbitals (B), and finally the $3z^2 - r^2$ orbital (C), at energies that we denote by E_{xy}, $E_{yz,zx}$, and E_{z^2}. These orbital assignments were obtained by interpreting the angular and polarization dependence of the RIXS spectra, as done in detail by Moretti Sala *et al.*[19] Moreover these assignments are corroborated by the results of *ab initio* quantum chemical calculations published by some of us[10] and by those given hereafter.

We first focus on the orbital excitation A from $x^2 - y^2$ to xy at energy E_{xy}, whose dependence on the average lattice parameter is given by the spectra of Fig. 2(b). Empirically we find that the fractional variations of both orbital energy ($|\delta E_{xy}/E_{xy}|$) and lattice parameter ($\delta a/a_0$) are linear in the film thickness s to the power −0.7 [Figs. 2(d) and 2(e)]. By combining the two dependencies, i.e., by eliminating s, and by noting that δE is negative for tensile strain, we can retrieve the linear relationship of Eq. (1), i.e. $(\delta E_{xy}/E_{xy}) = -n_{xy}\cdot(\delta a/a_0)$ with $n_{xy} = 4.1 \pm 0.45$. Given above considerations, the coefficient n_{xy} is also the exponent in the power law dependence of the type $E \propto a^{-n}$, where a is the average lattice parameter. The extracted exponents for the two other orbital excitations are also close to this value ($n_{yz,zx} = 3.8 \pm 0.55$ and $n_{z^2} = 3.95 \pm 0.55$).

It is noteworthy that the point representing compression [green in Figs. 2(d) and 2(e)] is within the error bars on the same trend of the tensile effect: This is due to the fact that we are in the limit of small deformations, as confirmed by the calculations given below; obviously at higher deformations an asymmetry between compressive and tensile strain is expected. Following the same procedure for the magnon we find an exponent that is about twice as large $n_M = 8.2 \pm 2.5$ with a much bigger uncertainty, due to the lower energy of the magnetic excitation which makes the analysis more difficult.

B. Quantum chemical calculations

To cross fertilize theory and experiment and to achieve a quantitative comparison of the theoretical exponents with the experimental ones, we rely on a real-space methodology, which in the spirit of modern multiscale electronic structure approaches describes a given region around a central Cu site by advanced quantum chemical many-body techniques, while the remaining part of the solid is modeled on a less sophisticated level. The treatment takes into account phenomenologically the strain by inserting in the calculations the experimental values of the average lattice parameter. This greatly simplifies the problem and is a good approach, as it is shown below. The cross talking between the CuO_2 planes is negligible so that the c parameter is not relevant, but in any case we used the experimental values. Moreover the exponent of the magnetic excitations is calculated by considering the lattice parameter dependence of the first neighbors superexchange, i.e., by neglecting next neighbors and cyclic interactions;[26,27]

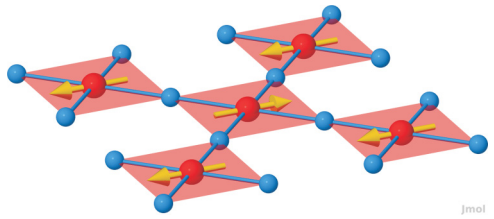

FIG. 3. (Color online) Five-plaquette fragment used in the embedded-cluster quantum chemical calculations (the eight Ca^{2+} ions above and below the CuO_2 planes are not shown).

the comparison between data and theory given below shows that this is sufficient to our purposes, at least with the present error bars in the experiment.

With quantum chemistry methods we calculated both the orbital splittings[10,28,29] and the nearest neighbor exchange constant J.[30] The complete-active-space self-consistent-field (CASSCF) method was used to generate multiconfigurational wave functions and it accounts for the strong correlation effects. Weaker correlations are subsequently treated by carrying out multireference second-order perturbation theory (CASPT2) calculations.[9] The d-d excitation energies are calculated on clusters consisting of five CuO_4 plaquettes, as in Fig. 3, and eight Ca ions (not shown) with a point-charge embedding. For additional insights into the dependence on strain of J, CASSCF and CASPT2 computations were further carried out on smaller, two-plaquette embedded clusters.

C. Discussion

The calculated ground state and d-d excitation energies are compared directly with the experimental values in Figs. 4(a) and 4(b). As for other two dimensional cuprates[10] the absolute values of the excitation energies in the unstrained CCO system match the experimental ones rather well, within 2% for E_{xy} and 8% for E_{z^2}. The deviation in absolute value for $E_{yz,zx}$ is somewhat larger, but the important observation is that the calculated slope, and thus the exponent, match the experimental one. Indeed we find all orbital exponents to be close to four, as they are in the experiment. Regarding the magnetic excitations the calculations give a superexchange $J = 132$ meV for the relaxed CCO that scales under strain with an exponent 7.45, again close to the experimental value of 8.2. Theoretical exponents are also given by the red bars in Fig. 4(d) compared with the experiment (black dots). We note here that also the calculated total electronic energies [Fig. 4(c)] are satisfactory since they give a minimum close to the experimental value of the lattice parameter of the relaxed system.

The same calculated total energies of Fig. 4(c) shed light onto the mechanism of the strain effect. When the strain modifies the lattice parameter, the computed total energy goes away from the minimum and this change is compensated by the elastic energy accumulated in the system and not included in the calculation. Both the initial and the final states of the transition change considerably in energy by almost the same amount, so that the displacement of the spectra and the measured variation of the transition energy is a tiny difference [in blue in Fig. 4(c)], which results

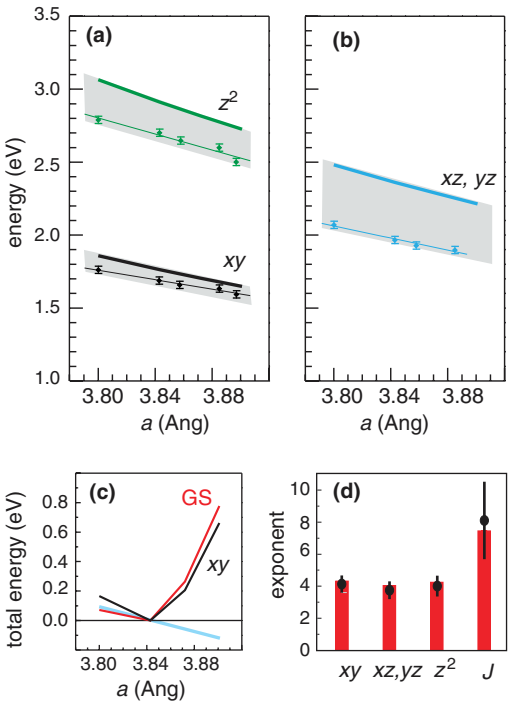

FIG. 4. (Color online) (a)(b) Orbital excitation energies vs average lattice parameter a: comparison between RIXS experimental (square data points) and computational (heavy lines) results. (c) Calculated total energies vs lattice parameter: ground state (GS, in red), xy excited state (in black), and difference in blue. (d) Comparison between theoretical exponents (red bars) and experimental values (black dots) in the $E \propto 1/a^n$ power law of orbital and magnetic excitation energies.

linear versus the lattice parameter. The agreement between theory and experiment in the exponents demonstrates the quality of the quantum chemistry calculations. Moreover it shows that the approach of inserting the experimental values of the lattice parameter in a calculation not including the elastic energy is very satisfactory. The experimental error bars and the limitations coming from the smallness of the cluster, unavoidable in feasible calculations, do not allow the discussion of the differences between the exponents of the three orbital excitations; nonetheless it is comfortable that the exponent of the xy excitation is the highest as expected, being an effect within the CuO_2 plane. We also note that the quantum chemistry methods used do not include interface effects, such as charge accumulation. However the success of the calculations strongly suggests that these effects are not relevant to the problem addressed here. We summarize all experimental and theoretical values of the exponents in Table I.

The observed exponents can be analyzed in terms of a simplified three-band Hubbard model description of cuprates, in which the Cu $3d$ - O $2p$ hopping integral, t_{pd}, plays an essential role in determining both the superexchange[31–33] and the covalent contribution E to the crystal-field splitting of the orbital energies.[34,35] In the strong coupling Mott insulating regime the superexchange is proportional to $(t_{pd})^4$ and the covalent contribution to t_{pd} at a power between 1 and 2. On the other hand for materials with a small charge transfer energy

TABLE I. All calculated and experimental scaling exponents for orbital (n_{xy}, $n_{xz,yz}$, n_{z^2}) and magnetic (n_M) excitations. Note that, while the experimental exponent n_M comes from the scaling of the magnon peak, the calculated one comes from the scaling of the first neighbors superexchange J.

	n_{xy}	$n_{xz,yz}$	n_{z^2}	n_M
Exp.	4.1 ± 0.45	3.8 ± 0.55	3.95 ± 0.55	8.2 ± 2.5
Calc.	4.30	4.12	4.25	7.45

Δ one finds E proportional to t_{pd} and for large Δ instead E is proportional to $(t_{pd})^2/\Delta$. On this basis one expects a ratio of magnetic and orbital exponent between 2 and 4, which matches both the experimental (on average $n_M/n_{\rm orb} = 2.08$) and *ab initio* (1.76) findings. Vice versa by describing the hopping with a power law ($1/a^\eta$), the observed exponents imply that $\eta \approx 2$, which is smaller than previous, less refined, theoretical estimates[20,36] giving η in the interval 3–4.

IV. CONCLUSIONS

We have hereby not only established and quantified the strain-induced modifications of two fundamental energy scales in the insulating model system CCO, but also provided as a general guideline a scaling directly relevant in the context of high-T_c superconductivity in copper oxides, particularly for pairing mechanisms relying on magnetic interactions where J is a key parameter. Obviously the present results are directly pertinent to the superconductivity observed in CCO/STO heterostructures.[13] On the other hand, if more specific information on a particular system is needed, the present work is also of importance. In fact it demonstrates that modern RIXS makes it possible to investigate the relevant energy scales with relatively simple experiments.

Moreover a clear comprehension of the scaling of orbital excitations could be crucial as well. In fact it has been recently suggested[37] that the critical temperature T_c is highly sensitive to the d-level splitting E_{z^2} and that the off-diagonal coupling between $x^2 - y^2$ and z^2 symmetry states substantially affects the dispersion of the low-energy bands and the shape of the Fermi surface.[38–40] These orbital splittings are also essential for proposed excitonic mechanisms for pairing and high-T_c superconductivity.[41] Finally we note also that the computational approach presented here, now validated by the experiment, can be used also in computer experiments and offers an opportunity to expand the work on strain-engineering of copper-oxide materials.

ACKNOWLEDGMENTS

This research project has been partially supported by the Italian Ministry of Research MIUR (Grant No. PRIN-20094W2LAY).

APPENDIX

1. The samples characterization

The samples were grown by laser ablation, and the details are given in Ref. 22. Immediately after the preparation in Roma Tor Vergata, i.e., before the RIXS measurements, the samples were characterized by conventional x-ray diffraction and kept in inert atmosphere up to the RIXS measurements at the Swiss Light Source. Successively they were transferred to the European Synchrotron Radiation Facility in Grenoble, where a more detailed characterization with synchrotron radiation has been done, together with measurements on reference samples grown to this purpose in the same way. In particular diffraction patterns were recorded at the ID03 beamline at the same temperature used in the RIXS experiment, i.e., 15 K, so the data could be safely combined. The aim was to determine the average lattice parameter in the ab plane and the thickness of the films and to test their quality, as detailed hereafter.

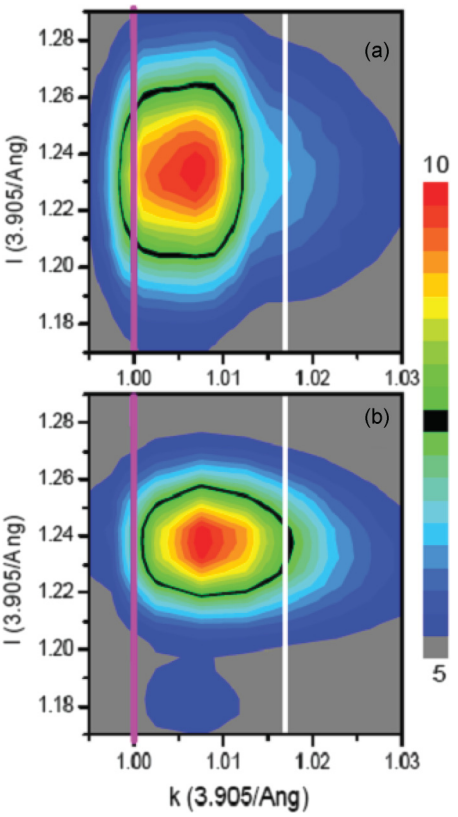

FIG. 5. (Color online) Diffraction maps from $CaCuO_2$ on $SrTiO_3$: The thickness of the overlayer is 60 Å (a) and 102 Å (b), respectively.

The samples have been prepared without capping since an overlayer can interdiffuse, as we have seen in preliminary experiments; for this reason stocking in inert atmosphere is important. The crystallographic investigation is based on diffraction maps, as the ones shown in Fig. 5.

The maps in the reciprocal space are plotted as a function of the Miller indices k and l in units normalized to the $SrTiO_3$ substrate. Thus the magenta line corresponds to the $SrTiO_3$ lattice parameter, i.e., to the strained CCO and the white line to the fully relaxed CCO. Note that the rocking curves constituting the maps are rather broad, due to the small number of unit cells in the film thickness. As a consequence in the maps the tails of the diffraction peaks extend largely beyond the white vertical line. With this precaution in mind the comparison between the maps from films of different thickness is illuminating. This is done in Fig. 5 for the samples with

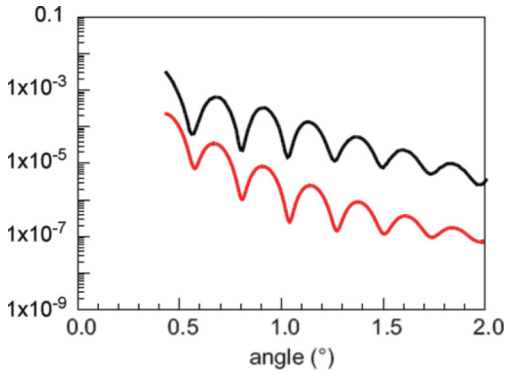

FIG. 6. (Color online) Oscillations of the x-ray reflectivity at 15 KeV from the CCO/$SrTiO_3$ system with overlayer thickness 102 Å. The theoretical reflectivity is plotted in red and it is to scale, while the experimental one (in black) is given apart an arbitrary scale factor.

thickness equal to 60 Å [panel (a)] and 102 Å [panel (b)], respectively. The black belt in the maps represents the half height, and the gray area corresponds to 5% of the maximum (the photon energy is 15 keV). The shape of the two maps is very different and the partial relaxation of the thicker film is very clear. On the other hand most of the intensity of the map relative to the 60 Å sample is concentrated at small k (i.e., larger values of the lattice parameter a), indicating a considerable strain.

The other issue is the determination of the thickness and the evaluation of the roughness of the films. This is done with the oscillations of the reflectivity versus the angle of incidence in grazing conditions. We did not try to calibrate the reflectivity in absolute terms since this is irrelevant to our purposes. As an example we consider the 102 Å thick film: Many oscillations are well seen in the logarithmic plot of Fig. 6, indicating a high quality film (black curve). A fitting as the one in Fig. 6 (red curve), with the inclusion of roughness factor[42] and Gaussian smoothing, reproduces very well the experimental trend and gives a roughness around 4 Å, i.e., slightly more than a CCO unit cell. This is similar to the one obtained for other high quality films prepared by PLD, as, for example, the largely studied $LaAlO_3/SrTiO_3$ heterostructure.[43–45] This is not surprising since the CCO samples for the present experiment have been grown with the same experimental apparatus used to grow CCO/STO superlattices[13] which show neat and sharp interfaces, as displayed in the HRTEM image of Ref. 13. Note that in the log plot the reflectivity scale is appropriate to the red theoretical curve. The measured curve (in black) instead is defined apart a factor, i.e., a rigid vertical translation in logarithmic scale, and its position in the graph has been chosen simply for readability.

2. *Ab initio* calculation of superexchange and orbital excitation energies

All calculations were performed with the MOLCAS quantum-chemistry package.[46] In the CASSCF and CASPT2 computations of Cu d-level splittings (see main text), we can evenly describe the strong on-site d-shell correlations as well as the intersite d-p and d-p-d couplings, since the four nearest-neighbor (NN) plaquettes around a central CuO_4 unit are explicitly included at the all-electron level. For those 5-plaquette clusters, quadruple-zeta valence basis sets plus polarization functions were used for the Cu and O ions of the central plaquette and double-zeta basis sets for Cu and O sites at the four adjacent plaquettes and at the Ca NN's. On the other hand quadruple-zeta valence basis sets plus polarization functions were employed for the Cu and O ions of the smaller two-plaquettes fragments and double-zeta basis sets for the Ca NN's. In each case, the farther Cu neighbours are modeled with total-ion effective potentials.[47] The remaining part of the solid-state matrix is always described by large arrays of point charges, fitted to reproduce the Madelung field within the cluster region. In the CASPT2 calculations, we correlated all Cu $3d$ and O $2p$ orbitals.

*Present address: European Synchrotron Radiation Facility, 6 rue Jules Horowitz, F-38043 Grenoble, France.

[1]See, for instance, N. Plakida, *High Temperature Cuprate Superconductors* (Springer Publishers, Heidelberg, 2010).

[2]J. H. Haeni, P. Irvin, W. Chang, R. Uecker, P. Reiche, Y. L. Li, S. Choudhury, W. Tian, M. E. Hawley, B. Craigo, A. K. Tagantsev, X. Q. Pan, S. K. Streiffer, L. Q. Chen, S. W. Kirchoefer, J. Levy, and D. G. Schlom, Nature (London) **430**, 758 (2004).

[3]R. J. Zeches, M. D. Rossell, J. X. Zhang, A. J. Hatt, Q. He, C.-H. Yang, A. Kumar, C. H. Wang, A. Melville, C. Adamo, G. Sheng, Y.-H. Chu, J. F. Ihlefeld, R. Erni, C. Ederer, V. Gopalan, L. Q. Chen, D. G. Schlom, N. A. Spaldin, L. W. Martin, and R. Ramesh, Science **326**, 977 (2009).

[4]J. Chakhalian, J. M. Rondinelli, Jian Liu, B. A. Gray, M. Kareev, E. J. Moon, N. Prasai, J. L. Cohn, M. Varela, I. C. Tung, M. J. Bedzyk, S. G. Altendorf, F. Strigari, B. Dabrowski, L. H. Tjeng, P. J. Ryan, and J. W. Freeland, Phys. Rev. Lett. **107**, 116805 (2011).

[5]J.-P. Locquet, J. Perret, J. Fompeyrine, E. Mächler, J. W. Seo, and G. Van Tendeloo, Nature (London) **394**, 453 (1998).

[6]T. Siegrist, S. M. Zahurak, D. W. Murphy, and R. S. Roth, Nature (London) **334**, 231 (1988).

[7]L. Braicovich, L. J. P. Ament, V. Bisogni, F. Forte, C. Aruta, G. Balestrino, N. B. Brookes, G. M. De Luca, P. G. Medaglia, F. Miletto Granozio, M. Radovic, M. Salluzzo, J. van den Brink, and G. Ghiringhelli, Phys. Rev. Lett. **102**, 167401 (2009).

[8]L. J. P. Ament, Michel van Veenendaal, T. P. Devereaux, J. P. Hill, and J. van den Brink, Rev. Mod. Phys. **83**, 705 (2011).

[9]T. Helgaker, P. Jørgensen, and J. Olsen, *Molecular Electronic-Structure Theory* (Wiley, Chichester, 2000).

[10]L. Hozoi, L. Siurakshina, P. Fulde, and J. van den Brink, Sci. Rep. **1**, 65 (2011).

[11]S. Y. Savrasov and O. K. Andersen, Phys. Rev. Lett. **77**, 4430 (1996).

[12]P. Zhang, S. G. Louie, and M. L. Cohen, Phys. Rev. Lett. **98**, 067005 (2007).

[13]D. Di Castro, M. Salvato, A. Tebano, D. Innocenti, C. Aruta, W. Prellier, O. I. Lebedev, I. Ottaviani, N. B. Brookes, M. Minola, M. Moretti Sala, C. Mazzoli, P. G. Medaglia, G. Ghiringhelli,

L. Braicovich, M. Cirillo, and G. Balestrino, Phys. Rev. B **86**, 134524 (2012).
[14]H. Zhang, Y. Y. Wang, H. Zhang, V. P. Dravid, L. D. Marks, P. D. Han, D. A. Payne, P. G. Radaelli, and J. D. Jorgensen, Nature **370**, 352 (1994).
[15]S. Tao and H.-U. Nissen, Phys. Rev. B **51**, 8638 (1995).
[16]L. Braicovich, J. van den Brink, V. Bisogni, M. Moretti Sala, L. J. P. Ament, N. B. Brookes, G. M. De Luca, M. Salluzzo, T. Schmitt, V. N. Strocov, and G. Ghiringhelli, Phys. Rev. Lett. **104**, 077002 (2010).
[17]M. Le Tacon, G. Ghiringhelli, J. Chaloupka, M. Moretti Sala, V. Hinkov, M. W. Haverkort, M. Minola, M. Bakr, K. J. Zhou, S. Blanco-Canosa, C. Monney, Y. T. Song, G. L. Sun, C. T. Lin, G. M. De Luca, M. Salluzzo, G. Khaliullin, T. Schmitt, L. Braicovich, and B. Keimer, Nat. Phys. **7**, 725 (2011).
[18]J. Schlappa, K. Wohlfeld, K. J. Zhou, M. Mourigal, M. W. Haverkort, V. N. Strocov, L. Hozoi, C. Monney, S. Nishimoto, S. Singh, A. Revcolevschi, J.-S. Caux, L. Patthey, H. M. Rønnow, J. van den Brink, and T. Schmitt, Nature (London) **485**, 82 (2012).
[19]M. Moretti Sala, V. Bisogni, C. Aruta, G. Balestrino, H. Berger, N. B. Brookes, G. M. de Luca, D. Di Castro, M. Grioni, M. Guarise, P. G. Medaglia, F. Miletto Granozio, M. Minola, P. Perna, M. Radovic, M. Salluzzo, T. Schmitt, K. J. Zhou, L. Braicovich, and G. Ghiringhelli, New J. Phys. **13**, 043026 (2011).
[20]W. A. Harrison, *Electronic Structure And The Properties Of Solids* (Freeman, San Francisco, 1980).
[21]O. Andersen, Phys. Rev. B **12**, 3060 (1975).
[22]G. Balestrino, R. Desfeux , S. Martellucci, A. Paoletti, G. Petrocelli, A. Tebano, B. Mercey, and M. Hervieu, J. Mater. Chem. **5**, 1879 (1995).
[23]V. N. Strocov, T. Schmitt, U. Flechsig, T. Schmidt, A. Imhof, Q. Chen, J. Raabe, R. Betemps, D. Zimoch, J. Krempasky, X. Wang, M. Grioni, A. Piazzalunga, and L. Patthey, J. Synchrotron Rad. **17**, 631 (2010).
[24]G. Ghiringhelli, A. Piazzalunga, C. Dallera, G. Trezzi, L. Braicovich, T. Schmitt, V. N. Strocov, R. Betemps, L. Patthey, X. Wang, and M. Grioni, Rev. Sci. Instrum. **77**, 113108 (2006).
[25]L. Braicovich, M. Moretti Sala, L. J. P. Ament, V. Bisogni, M. Minola, G. Balestrino, D. Di Castro, G. M. De Luca, M. Salluzzo, G. Ghiringhelli, and J. van den Brink, Phys. Rev. B **81**, 174533 (2010).
[26]R. Coldea, S. M. Hayden, G. Aeppli, T. G. Perring, C. D. Frost, T. E. Mason, S.-W. Cheong, and Z. Fisk, Phys. Rev. Lett. **86**, 5377 (2001).
[27]B. Dalla Piazza, M. Mourigal, M. Guarise, H. Berger, T. Schmitt, K. J. Zhou, M. Grioni, and H. M. Rønnow, Phys. Rev. B **85**, 100508 (2012).
[28]C. de Graaf and R. Broer, Phys. Rev. B **62**, 702 (2000).
[29]H.-Y. Huang, N. A. Bogdanov, L. Siurakshina, P. Fulde, J. vanden Brink, and L. Hozoi, Phys. Rev. B **84**, 235125 (2011).
[30]D. Muñoz, F. Illas, and I. de P. R. Moreira, Phys. Rev. Lett. **84**, 1579 (2000).
[31]P. W. Anderson, Phys. Rev. **79**, 705 (1950).
[32]J. Zaanen and G. A. Sawatzky, Can. J. Phys. **65**, 1262 (1987); J. Zaanen and A. M. Oleś, Phys. Rev. B **37**, 9423 (1988).
[33]F. Barriquand and G. A. Sawatzky, Phys. Rev. B **50**, 16649 (1994).
[34]P. W. Anderson, Phys. Rev. **115**, 2 (1959).
[35]E. Dagotto, Rev. Mod. Phys. **66**, 763 (1994).
[36]W. Weber, Phys. Rev. Lett. **58**, 1371 (1987).
[37]H. Sakakibara, H. Usui, K. Kuroki, R. Arita, and H. Aoki, Phys. Rev. Lett. **105**, 057003 (2010); Phys. Rev. B **85**, 064501 (2012).
[38]H. Eskes and G. A. Sawatzky, Phys. Rev. B **44**, 9656 (1991).
[39]E. Pavarini, I. Dasgupta, T. Saha-Dasgupta, O. Jepsen, and O. K. Andersen, Phys. Rev. Lett. **87**, 047003 (2001).
[40]L. Hozoi, M. S. Laad, and P. Fulde, Phys. Rev. B **78**, 165107 (2008).
[41]W. A. Little and M. J. Holcomb, J. Supercond. **13**, 695 (2000).
[42]L. Nevot and P. Croce, Revue Phys. Appl. **15**, 761 (1980).
[43]P. R. Willmott, S. A. Pauli, R. Herger, C. M. Schleptz, D. Martoccia, B. D. Patterson, B. Delley, R. Clarke, D. Kumah, C. Cionca, and Y. Yacoby, Phys. Rev. Lett. **99**, 155502 (2007).
[44]T. Fix, F. Schoofs, J. L. MacManus-Driscoll, and M. G. Blamire, Phys. Rev. Lett. **103**, 166802 (2009).
[45]Y. Chen, N. Pryds, J. E. Kleibeuker, G. Koster, J. Sun, E. Stamate, B. Shen, G. Rijnders, and S. Linderoth, Nano Lett. **11**, 3774 (2012).
[46]MOLCAS7, University of Lund, Sweden (www.molcas.org).
[47]F. Illas, J. Rubio, and J. C. Barthelat, Chem. Phys. Lett. **119**, 397 (1985).